

## Chapter 8 Fold-change detection

### 8.1 Universal features of sensory systems

Sensory systems in animals like vision and hearing and sensory systems of cells like bacterial chemotaxis share universal features. One of these features is exact adaptation, which, as we saw in the previous chapter, is the ability to adjust to the background signal. When we go from sunlight into a dark room lit by a candle, at first we don't see very well but after a while our pupils dilate to let in more light and our eyes adjust.

A second universal feature is sensing of **relative changes** rather than absolute changes. Suppose that we adapt to our room lit by a candle, and then we add a second candle. We sense a large change in light. But if we add the same candle to room lit by a chandelier with 50 candles, we barely notice the change. The absolute number of photons added is the same, one candle's worth, but the relative change is very different.

Historically, response to relative changes, also known as **Weber's law**, was first described in human senses such as weight perception. Weber, in the 19<sup>th</sup> century, let people hold a weight  $x_0$  for a while, and then slowly added small weights to measure the minimal detectable increase  $\Delta x_{\min}$ , at which people first felt the extra weight. It turns out that the minimal detectable increase was proportional to the initial weight  $x_0$ ,  $\Delta x_{\min} = k x_0$ , where  $k$  is Weber's constant ( $k \sim 0.1$  for weight perception,  $k$ ). You can detect 10g on the background of 100g, but you only detect 100g on a background of 1 kilo. In all cases, sensing of relative changes is found for a range of several decades of input signal (typically 2-5). Relative sensing is lost at very weak signal on the brink of detection or very strong signals that saturate the receptors.

Even psychological senses seem to work on relative changes. For example, psychologists measure subjective well-being using carefully designed questionnaires. Each person has an individual steady-state level of well-being. Positive events such as getting a raise in salary raise well-being for a while, but then well-being adapts back exactly to baseline. The immediate change in well-being seems to depend on relative changes. If you have been earning 10\$ a week, a 10\$ raise is cause for celebration. If you have been earning 1000\$ a week, a 10\$ raise will go almost unnoticed.

Many sensory systems of cells also show these universal features - exact adaptation and sensing of relative changes. For cells, as well as for animals, sensing relative changes is important in order to be robust to the noise in the input. To respond correctly, the cell must tell the difference between a true input signal and noise. Suppose that a cell senses a signal molecule by means of receptors. It suddenly experiences an increase of

10 binding events per second of the signal molecule to the receptors. Is this a true signal or just noise?

The answer depends on the background level of the input signal – or in other words, on the recent context of the signal. If the cell has been sitting for a while in a background of 1 binding event per second, a rise of 10/sec is an eyebrow-raising 10-fold increase, and is likely to be important. If instead the cell has been soaking in 1000 binding events/sec, the same increase of 10/sec is tiny (even smaller than the typical noise of  $\sqrt{1000} \sim 30$  mol/sec), and should be rejected as a fluctuation. Thus, decisions had best be based on *relative* changes, not absolute changes.

In this chapter we will see how relative changes are sensed. We will begin with the system we studied in the last chapter, bacterial chemotaxis, because the circuit is well understood. We will then ask which kinds of circuits in general can sense relative changes.

### Fold-change detection in bacterial chemotaxis

The chemotaxis system of *E. coli*, the navigation system that allows bacteria to climb gradients of attractant, can sense relative changes across several orders of magnitude of background signal. This wide dynamic range was discovered by Mesibov, Ordal and Adler (1973). They placed swimming *E. coli* in a dish and let them adapt to a background level  $S_0$  of the attractant alpha-methyl aspartate.

Then they place a pipette with attractant concentration 3.2 times  $S_0$  into the dish (Fig 8.1). The experimenters repeated this experiment with different levels of  $S_0$ . The number of bacteria that swam into the pipette in an hour was roughly the same across three orders of magnitude of attractant levels (Fig 8.2). It made no

difference whether concentrations were in micromolar or millimolar, bacteria could still detect the 3.2-fold higher concentration of attractant in the pipette.

A more direct test for relative sensing in bacterial chemotaxis was presented by Lazova and Tom Shimizu []. They used a microfluidic device to present *E. coli* cells with time

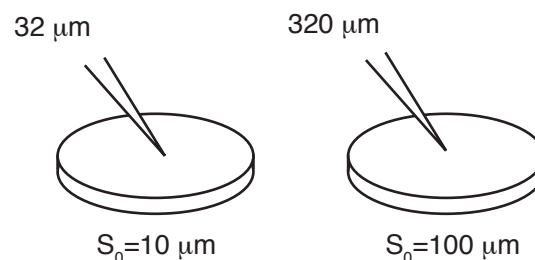


Figure 8.1

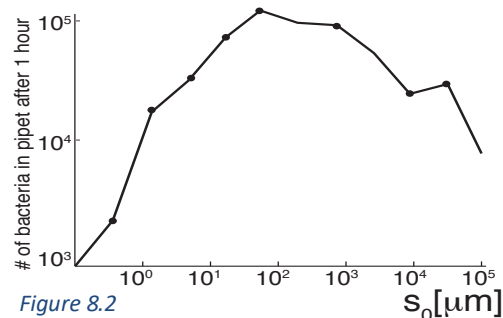


Figure 8.2

concentration of the attractant alpha-methyl aspartate, the input signal  $S(t)$ . The signals were all based on the same pattern:  $S(t)$  started at a background level  $S_0$  and then wiggled up and down. Then they multiplied the same signal, including its background, by a factor  $\lambda$ . In this way, the presented the bacteria with a series of signals had a scale  $\lambda$  that ranged across several orders of magnitude. This experimental design provided input signals with the same fold change  $F(t)=S(t)/S_0$  but very different absolute changes (Fig 8.3).

Lazova and Shimizu measured the chemotaxis output, which we denote  $a(t)$ , using a fluorescence system developed by Sourjik and Berg, in which the interaction of CheY and flagellar motor is accurately visualized using fluorescence energy transfer (FRET)[]. They found that the output was invariant to the multiplicative constant  $\lambda$ , across three decades of background concentration from about 20uM to 3 mM of attractant. Bacterial chemotaxis shows senses relative changes.

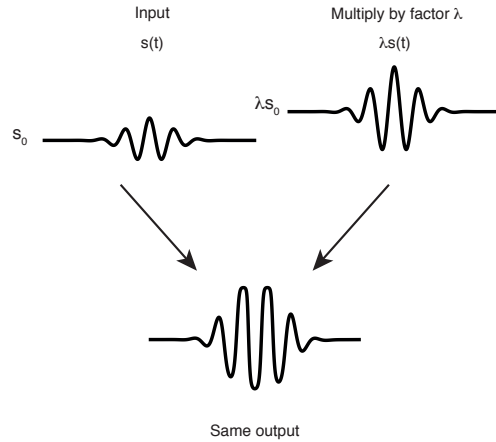


Figure 8.3

**Definition of fold change detection (FCD)**

Let's define what we mean by sensing relative changes more precisely. We want the entire shape of the output curve to depend only on the signal normalized to its background, which is called the fold-change of the signal. Consider a system with output  $a(t)$  that is adapted to a background signal  $S_0$ . Now let the signal change  $S(t)$ . We define **Fold change detection (FCD)** as a response curve  $a(t)$  whose entire shape- including peak amplitude and response time- depends only on the relative change in input  $S(t)/S_0$ , and not on the absolute change. For example, an input step from level  $S=1$  to level  $S=2$  yields exactly the same

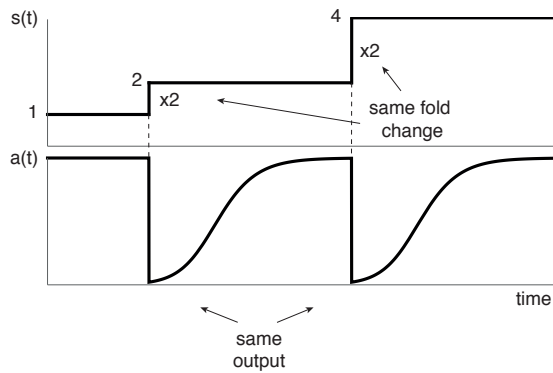


Figure 8.4

response curve as a step from 2 to 4 (Fig 8.4). This is because both steps have the same 2-fold change, even though the step from 2 to 4 is larger in absolute terms than the step

from 1 to 2. A step from 1 to 3 will yield a larger response, because the fold change is larger. A step from 3 to 9 will have a response identical to that of the step from 1 to 3.

If we present a system with FCD with a series of steps with the same absolute levels, say from 1 to 2 to 3 to 4, the response will diminish because the fold change gets smaller and smaller (Fig 8.5)

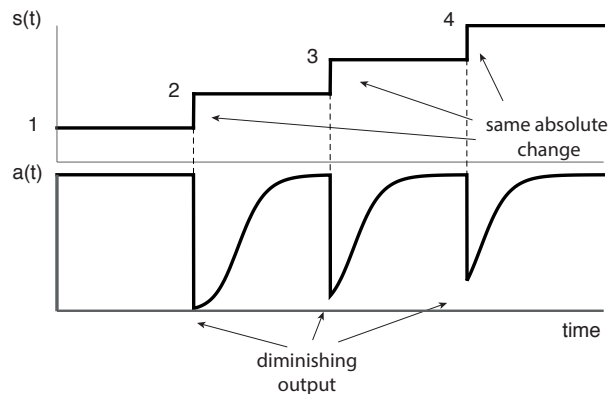


Figure 8.5

### The chemotaxis circuit provides FCD by means of a nonlinear integral feedback loop

Let's understand how bacterial chemotaxis achieves FCD. The intuitive mechanism is that output activity  $a(t)$  is a function of attractant signal  $S$  divided by its binding constant to the receptors  $K$ ,  $a=f(S/K)$ . The binding constant  $K$  rises proportionally to the background attractant signal thanks to the adaptation system. Thus, if input  $S$  is multiplied by  $\lambda$ , so is  $K$ , and hence  $f(S/K)$  remains unchanged.  $K$  is a slowly changing memory of previous signal that normalizes the signal scale out. Let's solve the chemotaxis model to see the origin of FCD.

**Solved example 1:** Show that the model for bacterial chemotaxis shows FCD

The equations for the model of bacteria chemotaxis (Eq 7X-X) have two variables: the normalized activity  $a$  (which sets the tumbling frequency), and the receptor binding constant  $K$  for the attractant  $S$ .

Activity  $a(t)$  is a Hill function of the attractant

$$(1) a=1/(1+(S/K)^n)=f(S/K)$$

The binding constant  $K$  is determined by the methylation reactions, which in turn depend only on activity  $a$ , providing integral feedback to the steady state activity  $a_{st}$ .

$$(2) dK/dt=K(a_{st}-a)$$

To reach  $a_{st}$ , Eq 2 adjusts  $K$  to match the background  $S_0$  so that  $f(S_0/K)=a_{st}$  (Fig 8.6). If we multiply  $S_0$  by  $\lambda$ , and let the system adapt, at steady-state  $K$  must also rise by a

factor of  $\lambda$ , so that the ratio  $S/K$  stays at the proper value  $f(\lambda S_0 / \lambda K) = f(S_0/K) = a_{st}$ . In other words, at steady-state  $K$  is proportional to the attractant background  $S_0$ ,  $K_{st} \sim S_0$ .

Now let  $S(t)$  change with time, resulting in an output  $a(t)$ . To prove FCD, we need to show that if we multiply  $S(t)$  by any positive constant  $\lambda$ , we still get the same output dynamics  $a(t)$ . To test this, we use **dimensional**

**analysis**, a useful technique that rescales  $S$  and  $K$  to dimensionless variables. We define the fold change as  $F(t) = S(t)/S_0$ , and the scaled binding constant as  $\tilde{K} = K/S_0$ . The re-scaled equations can be found by plugging in these new variables into eq x,y, to find

$$\frac{d\tilde{K}}{dt} = c\tilde{K}(a_{st} - a)$$

$$a = f\left(\frac{F(t)}{\tilde{K}}\right)$$

Note that  $S(t)$  does not appear in these equations, only the fold change  $F(t) = S(t)/S_0$ . Likewise,  $S$  does not appear in the initial conditions  $\tilde{K}(t=0)$  and  $F(t=0) = 1$ . Therefore, the output  $a(t)$  is not affected by multiplying  $S(t)$  by  $\lambda$ , because the fold  $F$  is unchanged. We conclude that the output  $a(t)$  is determined only by fold-change in input, hence FCD.

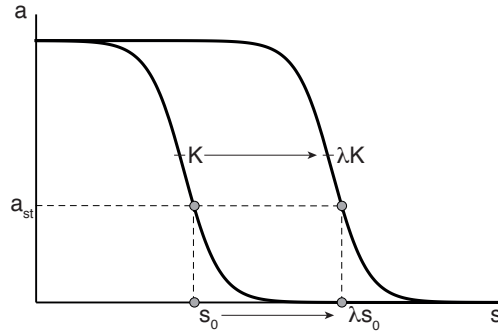


Figure 8.6

### 8.3 FCD and exact adaptation

Bacterial chemotaxis and the other sensory systems we mentioned show exact adaptation. In fact, any system with FCD must show exact adaptation. This is because if the output to a constant signal  $S_0$  is  $a_{st}$ , FCD demands that the output will be the same if we multiply  $S_0$  by any  $\lambda > 0$ . Thus, steady state output  $a_{st}$  is independent on the background signal, precisely the definition of exact adaptation.

However, exact adaptation is not enough to guarantee FCD. In fact, the best-known circuit for exact adaptation in engineering, linear integral feedback, does not show FCD, nor does any other linear circuit. This is because linear equations show output changes that are proportional to absolute (not relative) input changes (exercise 8.XX). The chemotaxis circuit shows FCD by virtue of the *non-linear* nature of its integral feedback loop, namely that  $dK/dt \sim K(a - a_{st})$  rather than the linear form  $dK/dt \sim a_{st} - a$ . That extra  $K$

gives a logarithmic flavor to the equations ( $d \log(K)/dt \sim \text{ast-a}$ ) needed to reject the input scale  $\lambda$ .

FCD is a pretty tough demand on a system- the entire dynamical response must depend only on fold change. Are there other circuits that can show FCD?

### 8.4 The incoherent FFL shows FCD

Intriguingly, demanding FCD narrows down the possible circuits to a very few. But among these few is a common network motifs. This motif is the incoherent type-1 FFL our old friend from chapter 4. It was the first circuit shown to have FCD, by Lea Goentoro and Marc Kirschner et al (Goentoro 2009)

In the I1FFL, input X activates both an output gene Z and its repressor Y. In chapter four, we modeled the I1FFL using logic input functions (AND and OR gates). To see its FCD property, we need more graded regulation. The I1FFL can provide FCD when (i) the binding of X to its promoters is weak (so that Michaelis-Menten terms become linear in  $X/(K_x+X) \sim X$ ), and (ii) binding of the repressor Y is strong (that is, when Y exceeds its binding constant  $K_y$  to the Z promoter,  $Y \gg K_y$ , so that the Michaelis-Menten binding term  $1/(1+Y/K_y)$  becomes, to a good approximation,  $K_y/Y$ ). In this case, we can write

$$(3) \frac{dy}{dt} = \beta_1 x - \alpha_1 y$$

$$(4) \frac{dz}{dt} = \frac{\beta_2 x}{y} - \alpha_2 z$$

After a step of x, z first rises, but then y rises and represses z production, forming a pulse of output z that adapts exactly to the previous steady state (Fig 8.7). As in chemotaxis, having a ratio  $x/y$  in the second equation normalizes out the input scale. In the following solved exercise we show that these equations have FCD, using dimensional analysis

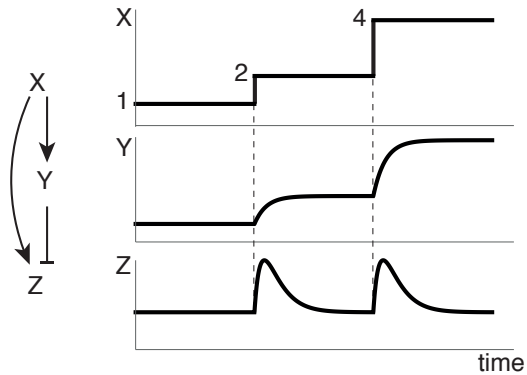


Figure 8.7

---

#### Solved example 1: IFFL can show FCD

Show that Eq. 3-4 show FCD.

Solution: First, let's see if the circuit has exact adaptation for the output Z. Let the system reach steady state for a constant input  $X_0$ . To see exact adaptation, we solve the steady-state condition  $dy/dt=0$ ,  $dz/dt=0$ . This yields  $Y_{st}=x_0/a_1$ , so that the repressor is

proportional to the background input. The output  $Z_{st}$  is  $Z_{st} = X_0 / y_{st} / a_2 = a_1 / a_2$ , which does not depend on input  $X_0$ . Thus  $Z$  shows exact adaptation.

Now let the input signal change,  $x(t)$ . To find the dynamics, let's define new variables, as we did for chemotaxis, by rescaling  $y$  to the steady-state input  $\tilde{y} = y / x_0$  and define the fold change  $F(t) = x(t) / x_0$ . In these new variables we get, by dividing Eq (3) by  $x_0$ , scaled equations that depend only on the fold change  $F(t)$ :

$$\frac{d\tilde{y}}{dt} = \beta_1 F - \alpha_1 \tilde{y}$$

$$\frac{dz}{dt} = \frac{\beta_2 F}{\tilde{y}} - \alpha_2 z$$

Thanks to exact adaptation, the initial conditions are independent on  $x_0$ . The dynamic equations are dependent only on fold change  $F$ , and thus the output dynamics  $Z(t)$  is completely determined only by fold-change in input, hence FCD.

FCD breaks down in the I1FFL when  $Y$  is too small to ignore the binding coefficient  $K_{yz}$  (exercise XX).

=====

FCD in the I1FFL circuit occurs for any value of the production and removal rates  $\alpha_{1,2}$  and  $\beta_{1,2}$  in Eq 3,4. These parameters affect the shape of the dynamics, by setting the amplitude and response time of the output pulse. Response times ranging from minutes to hours to days can be achieved by appropriate values of removal rates  $\alpha$ .

The I1FFL provides FCD because the repressor  $Y$  acts as an inner memory that records the previous background level. Multiplying the input  $x$  by  $\lambda$  leads to  $y$  dynamics also multiplied by  $\lambda$ , because Eq. 3 is linear. However,  $X$  and  $Y$  cancel each other out in the output dynamics because of the  $X/Y$  term in Eq. 4. This makes the output  $z$  independent on  $\lambda$  throughout the dynamics.

---



---

### A general condition for FCD

The two circuits we saw so far, I1FFL and NLIFBL, are the only FCD circuits that have been experimentally characterized in biological systems to date (Fig 8.8, note that node y in the NLIFBL has autoregulation because K in Eq 2 multiplies its own production rate). Are there other possible FCD circuits, and if so, how many? To address this, Oren Shoval and Eduardo Sontag et al (Shoval 2010) defined a useful **homogeneity condition** for FCD by which you can check equations for the FCD property. This condition generalizes the dimensionless variable approach we used for chemotaxis model and the IFFL. It requires that if the input is multiplied by a constant  $\lambda$ , the system has an internal variable y that also increases by a factor of  $\lambda$ . The inner variable y is used as a memory that divides the output z, normalizing out  $\lambda$ :

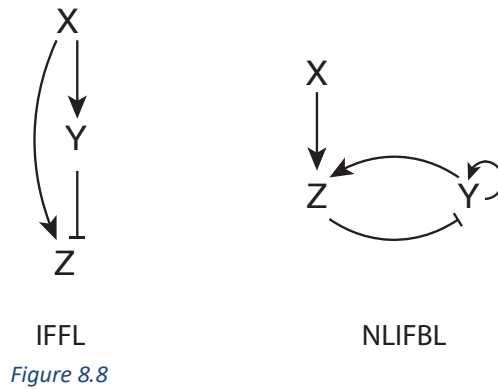


Figure 8.8

=====

**A general condition for FCD [Shoval et al:]**

Consider a system with input x, output z and internal variables y (Fig 8.9). The dynamics of y and z are given by the ordinary differential equations

$$dy/dt=f(x,y,z)$$

$$dz/dt=g(x,y,z)$$

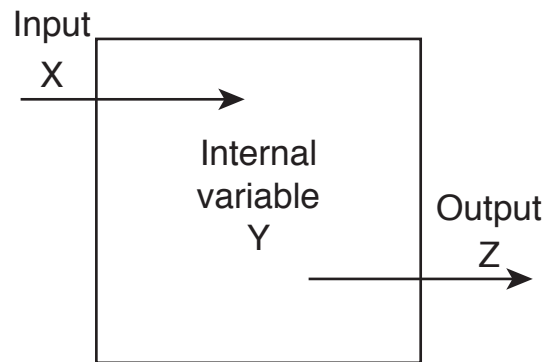


Figure 8.9

A sufficient condition for FCD is that the system is stable, that the output z shows exact adaptation, and that g and f satisfy the following homogeneity conditions for any  $\lambda > 0$  (a homogenous function of order m obeys  $h(\lambda x) = \lambda^m h(x)$ ).

$$f(\lambda x, \lambda y, z) = \lambda f(x, y, z)$$

$$g(\lambda x, \lambda y, z) = g(x, y, z)$$

If f is linear, the condition is also necessary.



The proof is essentially the same as for the solved examples above. A generalization in which  $y$  can depend more generally of  $\lambda$  is shown in Exc XX.

Both the chemotaxis and the I1FFL equations above satisfy these homogeneity conditions. For the IFFL, for example,  $f(x,y,z)=b_1x-a_2y$ , so that  $f(\lambda x, \lambda y, z)=\lambda f(x,y,z)$ . Similarly,  $g(x,y,z)=b_2x/y - a_2z$ , so that  $g(\lambda x, \lambda y, z)=g(x,y,z)$ . In the chemotaxis circuit  $f(S,K,a)=cK(a-a^*)$ , so that  $f(\lambda S, \lambda K, a)=\lambda f(S,K,a)$ . In contrast, linear integral feedback (without the  $K$  in front of the parenthesis) does not satisfy the conditions- it shows exact adaptation, but  $f(S,K,a)=c(a^*-a)$ , which fails the homogeneity test.

The conditions highlight that details are important for FCD. A different implementation of the I1FFL, called a sniffer[], in which  $Y$  inhibits  $Z$  not by transcription ( $dz/dt=x/y-z$ ) but by degradation ( $dx/dt=x-yz$ ) does not show FCD (Exercises). FCD is not found in the sniffer because response time depends on absolute (and not relative) input change.

-----

To look for new FCD circuits, Miri Adler and Avi Mayo et al (Adler 2017) used these homogeneity conditions to perform an analytic scan of a class of half-a-million three-node circuits (in this class, the conditions are necessary and sufficient). Only 0.1% of the circuits showed FCD, as opposed to 10% that showed exact adaptation. Due to the enormous number of circuits, this means several hundred FCD circuit topologies. Intriguingly, Adler et al showed that the two observed designs, I1FFL and non-linear integral feedback loop (NLIFBL), are among the handful of circuits that (i) have the minimal number of interactions and (ii) optimally trade-off performance in tasks such as large response amplitude and fast response time. All other minimal FCD circuits do worse on at least one task.

Often, FCD can be observed experimentally using input-output measurements, but the architecture of the underlying circuit is not fully known. Can one use dynamic measurements to tell if an FCD circuit is feedforward (an I1FFL) or feedback (like the chemotaxis circuit NLIFBL), even if the molecular players are not yet known? The answer is yes. I1FFL and NLIFBL differ, for example, in the way the output pulse amplitude depends on the fold change of an input a step: a non-cooperative I1FFL has a logarithmic dependence on fold and the NLIFBL a linear or power-law dependence (exercise xx) (Fig 8.XX). Interestingly, both circuits have a decreasing adaptation time with fold (exercise xx). Feedback and feedforward can also sometimes be distinguished by providing certain input signal 'acid-tests', such as pairs of input pulses (Exercise xx) (Rahi 2107).

Now that we understand the circuits that can provide FCD, and see that it is common in cellular and organismal sensing systems, we can return to the question of what FCD is good for.

### FCD provides robustness to input noise, and allows scale-invariant searches

One answer is that FCD helps sensory systems tell a true input from noise. FCD provides a truth detector. It responds only to changes that are on the same scale as the background, weeding out small fluctuations (Fig 8.10). FCD therefore allows a **wide input dynamic range**, by changing sensitivity according to background level, a feat which in engineering is called gain control. As we saw, FCD has another role: it makes the response robust to unwanted effects that multiply the input signal by a constant  $\lambda$  whose value cannot be known in advance. This solves a crucial problem in

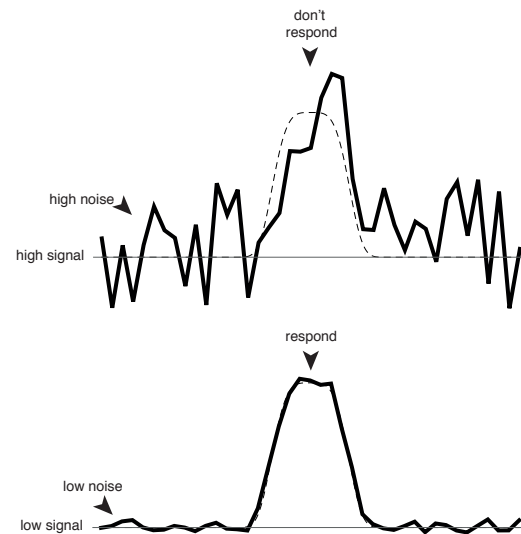


Figure 8.10

cells, as exemplified by an elegant experiment by Susan Gaudet and her students. Gaudet studied NF $\kappa$ B in mammalian cells, a transcription factor that responds to signals (such as tumor-necrosis factor, TNF), enters the nucleus and activates genes for inflammation and stress response. The readout of nuclear NF $\kappa$ B had better be accurate, so that cells can know whether to promote inflammation. Inflammation is a massive response that can fight pathogens, but causes collateral tissue damage and contributes to cancer and other diseases if it occurs at the wrong time.

The challenge for precise signaling is that there is a large variation between cells in the total level of NF $\kappa$ B protein. One cell might have 10,000 NF $\kappa$ B proteins and its neighbor cell might have 30,000. After a given TNF signal, the more NF $\kappa$ B a cell has, the more will enter the nucleus to activate genes. Thus, for the same signal, each cell will see a different amount of NF $\kappa$ B in the nucleus. In other words- an unknowable factor  $\lambda$  - the basal amount of NF $\kappa$ B in each individual cell - multiplies the amount of nuclear TF seen after a given signal. If the response of the downstream genes was absolute and not relative, the outcome would be disastrous: cells would arbitrarily make the wrong choices.

Gaudet showed that cells resolve this by using an I1FFL downstream of NFKb to respond only to fold-change in nuclear NFKb (Fig 8.11). The role of Y is played by inhibitors such as p50 that form dimers that compete with NFKb for the same site on target genes, and thus inhibits its effects. The I1FFL helps the cells to get used to the cell-specific level of NFKb and to normalize it out. Such buffering-out of multiplicative protein noise might help explain the prevalence of the I1FFL in transcription networks from bacteria to humans.

Multiplicative effects with an unknowable factor also occur in human vision. Here, the multiplicative factor is ambient light,  $L$ . Light levels can vary by almost ten orders of magnitude between midday and moonless night. Yet our eyes can see over much of this range. To understand the role of ambient light, imagine a visual search for a face in the crowd. We are interested in the contrast field  $R$  which carries information about the face. But our eyes see a light input that is the contrast  $R$  multiplied by the ambient light  $x=R L$ . To remove the multiplicative constant  $L$ , FCD in the visual system normalizes out the ambient light, and allows us to make an efficient search for a face that is invariant to a wide range of light levels.

Here is an interesting detail: at the level of the retina, there is no FCD because the neuronal output does not show exact adaptation but instead a steady-state level that is logarithmic in light  $L$ , providing the brain with information about ambient light. However, the full visual system does display exact adaptation, as shown by experiments that deviously move the visual field to cancel out our rapid eye movements called saccades. Thus, the subject sees a constant image. After a few seconds, the visual field seems to turn grey and vision stops working. We see thanks to the changes caused by rapid eye movements.

A similar multiplicative factor occurs in bacterial chemotaxis. Here the goal is to move towards sources of attractants, and the unknowable multiplying factor is the strength  $S_{\text{source}}$  of the attractant source. The concentration of attractant diffusing away from a source of strength  $S_{\text{source}}$  is proportional to  $S_{\text{source}}$ , due to the linearity of the diffusion (or convection) equation. Specifically, at position  $r$ , attractant levels are

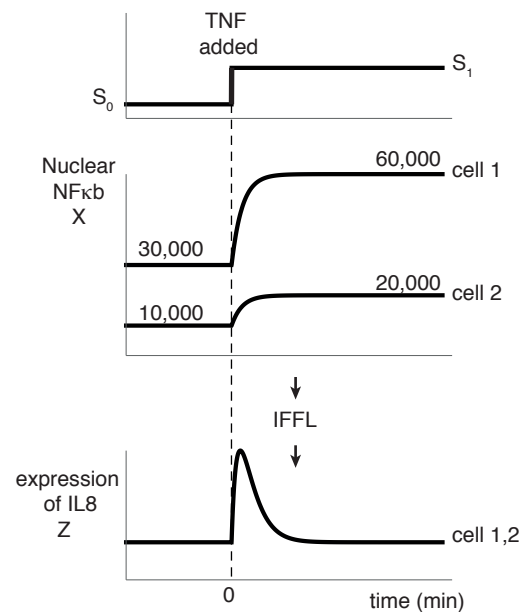


Figure 8.11

$S(r,t) = S_{\text{source}} \exp(-(r-r_0)^2/2Dt) / \sqrt{4\pi t}$ , which is proportional to  $S_{\text{source}}$ . Thanks to FCD, the navigating bacterium can show runs and tumble statistics that are invariant to  $S_{\text{source}}$  (as long as concentrations are in the range for FCD). The upshot is that bacteria can efficiently find the source position, regardless of the source strength. Such a process can explain the experiments of Mesibov et al with the pipette in the dish.

These properties of vision and chemotaxis can be called **scale-invariant search**, and are expected whenever an FCD system controls the movement of an agent in an input field plagued by an unknowable multiplicative factor.

In an imaginary experiment, a person searches for a cheesecake in a dark room using only the sense of smell. The room is in a cheesecake factory and has a certain background level of cheesecake aroma. After some sniffing around, the cake is found. Now do a search for half a cheesecake, but also halve the background level. If olfactory search is FCD, the average search time should be the same.

Fold-change detection is an instance where biological circuits evolved to 'learn' a scaling symmetry of the physical world: the multiplicative nature of ambient light, protein level or chemotaxis source strength. FCD makes the output invariant to the scalar multiplying the input. There are other possible symmetries and invariances to explore. For example, invariance in hormone circuits is explored in the next chapter. Such symmetries and invariances play a fundamental role in physics, and offer a field for further discovery in biology.